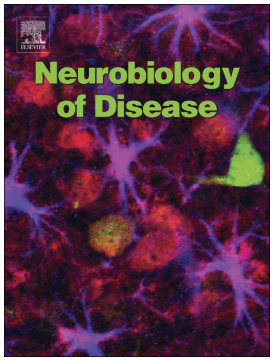

Neurogenesis upregulation on the healthy hemisphere after stroke enhances compensation for age-dependent decrease of basal neurogenesis

Joanna Adamczak, Markus Aswendt, Christina Kreutzer, Peter Rotheneichner, Adrien Riou, Marion Selt, Andreas Beyrau, Ulla Uhlenküken, Michael Diedenhofen, Melanie Nelles, Ludwig Aigner, Sebastien Couillard-Despres, Mathias Hoehn

PII: S0969-9961(16)30296-0
DOI: doi: 10.1016/j.nbd.2016.12.015
Reference: YNBDI 3882

To appear in: *Neurobiology of Disease*

Received date: 10 August 2016
Revised date: 12 December 2016
Accepted date: 18 December 2016

Please cite this article as: Joanna Adamczak, Markus Aswendt, Christina Kreutzer, Peter Rotheneichner, Adrien Riou, Marion Selt, Andreas Beyrau, Ulla Uhlenküken, Michael Diedenhofen, Melanie Nelles, Ludwig Aigner, Sebastien Couillard-Despres, Mathias Hoehn , Neurogenesis upregulation on the healthy hemisphere after stroke enhances compensation for age-dependent decrease of basal neurogenesis. The address for the corresponding author was captured as affiliation for all authors. Please check if appropriate. Ynbdi(2016), doi: 10.1016/j.nbd.2016.12.015

Neurogenesis upregulation on the healthy hemisphere after stroke enhances compensation for age-dependent decrease of basal neurogenesis

Joanna Adamczak[a, e, 1], Markus Aswendt[a,1], Christina Kreutzer[b,f], Peter Rotheneichner[b,f], Adrien Riou[a], Marion Selt[a], Andreas Beyrau[a], Ulla Uhlenküken[a], Michael Diedenhofen[a], Melanie Nelles[a], Ludwig Aigner[c,f], Sebastien Couillard-Despres[b,f], Mathias Hoehn[a,d,e,*]

[a] In-vivo-NMR Laboratory, Max Planck Institute for Metabolism Research, Gleuelerstrasse 50, 50931 Cologne, Germany

[b] Institute of Experimental Neuroregeneration, Spinal Cord Injury and Tissue Regeneration Center, Paracelsus Medical University Salzburg, Strubergasse 21, 5020 Salzburg, Austria

[c] Institute of Molecular Regenerative Medicine, Spinal Cord Injury and Tissue Regeneration Center, Paracelsus Medical University Salzburg, Strubergasse 21, 5020 Salzburg, Austria

[d] Department of Radiology, Leiden University Medical Center, Albinusdreef 2, 2333 ZA Leiden, The Netherlands.

[e] Percuros B.V., Enschede, Drienerlolaan 5-Zuidhorst, 7522 NB Enschede, The Netherlands.

[f] Spinal Cord Injury and Tissue Regeneration Center Salzburg (SCI-TReCS)

[1]These authors contributed equally.

* Address correspondence to:
Prof. Dr. Mathias Hoehn
In-vivo-NMR Laboratory
Max Planck Institute for Metabolism Research
Gleuelerstrasse 50
D-50931 Köln, Germany
Phone: +49-221-4726-315
Fax: +49-221-4726-337
Email: mathias@sf.mpg.de

Running title: Neurogenesis response to stroke in old mice

Abbreviations:

ANOVA – Analysis of variance, AUC – area under curve, Bioluminescence imaging – BLI, DCX – doublecortin, MRI – magnetic resonance imaging, M – months, MCAO – middle cerebral artery occlusion, NPC – neuronal precursor cell, SVZ – subventricular zone,

ABSTRACT

Stroke is a leading cause of death and disability worldwide with no treatment for the chronic phase available. Interestingly, an endogenous repair program comprising inflammation and neurogenesis is known to modulate stroke outcome. Several studies have shown that neurogenesis decreases with age but the therapeutic importance of endogenous neurogenesis for recovery from cerebral diseases has been indicated as its ablation leads to stroke aggravation and worsened outcome. A detailed characterization of the neurogenic response after stroke related to ageing would help to develop novel and targeted therapies. In an innovative approach, we used the DCX-Luc mouse, a transgenic model expressing luciferase in doublecortin-positive neuroblasts, to monitor the neurogenic response following middle cerebral artery occlusion over three weeks in three age groups (2, 6, 12 months) by optical imaging while the stroke lesion was monitored by quantitative MRI. The individual longitudinal and noninvasive time profiles provided exclusive insight into age-dependent decrease in basal neurogenesis and neurogenic upregulation in response to stroke which are not accessible by conventional BrdU-based measures of cell proliferation. For cortico-striatal strokes the maximal upregulation occurred at 4 days post stroke followed by a continuous decrease to basal levels by three weeks post stroke. Older animals effectively compensated for reduced basal neurogenesis by an enhanced sensitivity to the cerebral lesion, resulting in upregulated neurogenesis levels approaching those measured in young mice. In middle aged and older mice, but not in the youngest ones, additional upregulation of neurogenesis was observed in the contralateral healthy hemisphere. This further substantiates the increased propensity of older brains to respond to lesion situation. Our results clearly support the therapeutic relevance of endogenous neurogenesis for stroke recovery and particularly in older brains.

Keywords: stroke, neurogenesis, age dependence of neurogenesis after stroke, bioluminescence imaging, magnetic resonance imaging, doublecortin

INTRODUCTION

Adult neurogenesis in the neurogenic niches, namely the hippocampal subgranular zone and the subventricular zone (SVZ) of the lateral ventricles, continuously produces new cells for neuronal replacement in the hippocampus and the olfactory bulb (Garcia-Verdugo et al., 1998). However, endogenous neurogenesis declines with age (Ahlenius et al., 2009; Brown et al., 2003; Couillard-Despres et al., 2009; Hamilton et al., 2013; Luo et al., 2006). Age-dependent changes are detectable on all levels of neurogenesis, i.e. reduced numbers of neural stem cells (NSCs) (Enwere et al., 2004; Luo et al., 2006; Shook et al., 2012), decreased NSC proliferation, reduced neural progenitor cell and neuroblast proliferation (Tropepe et al., 1997) accompanied by structural changes of the SVZ architecture (Luo et al., 2006; Shook et al., 2012). The greatest reduction in cell genesis occurs between young adulthood and middle age with only modest additional decline during later senescence (reviewed in (Hamilton et al., 2013)).

Although adult neurogenesis by itself is not sufficient for complete recovery from brain injury such as stroke, its ablation aggravates infarct volume and worsens general stroke outcome (Butti et al., 2012; Sun et al., 2012; Wang et al., 2012). The endogenous NSCs represent an excellent therapeutic target for neurodegenerative diseases and provide the adult brain with a possibility of self-repair with low-level intervention (Lindvall and Kokaia, 2011). Pharmacological stimulation of endogenous neurogenesis with growth factors improved tissue replacement in rodent stroke models (Erlandsson et al., 2011; Kolb et al., 2007; Lai et al., 2008). It is therefore of high therapeutic relevance to better understand the mechanisms and dynamics of neurogenesis in response to brain injuries which widely lack effective treatments.

As neurodegenerative diseases or stroke occur predominantly in elderly people, the question arises whether endogenous neurogenesis of the aged brain is still beneficial despite its age-related decrease and if it can be employed for therapeutic interventions. Although the aged brain retains its capacity to respond with increased neurogenesis to brain injury (Darsalia et al., 2005; Jin et al., 2004), this response was reported in the rat to be altered in terms of intensity and timing (Jin et al., 2004; Sato et al., 2001). However, a clear description of the age-related changes in the neurogenic response to brain injury is not yet available, largely due to the situation that various studies investigated only discrete time points after stroke and

assessed different phases of neurogenesis (Jin et al., 2004; Sato et al., 2001; Takasawa et al., 2002; Tang et al., 2014).

Therefore, we followed the spontaneous neurogenic response to stroke at the level of doublecortin (DCX) expressing neuroblasts in three different age groups spanning the time period with the steepest decline in adult basal neurogenesis: 2, 6 and 12 months. In a novel approach, bioluminescence imaging was used to characterize the neurogenic response temporally and quantitatively *in vivo*. The DCX-Luc transgenic mice with luciferase gene expression restricted to neural progenitor cells allowed for repetitive measurements of individual animals. We used quantitative magnetic resonance imaging (MRI) to assess the stroke lesion over the experimental time period of 3 weeks in order to group animals based on similar ischemic territory. Using this noninvasive approach, we report here new insight into discriminating between the age dependent decline of neurogenesis and the neurogenic response to stroke. Our investigation contributes to the elucidation of important factors for recovery processes such as time window of maximal neurogenic response and contribution of subventricular zones on both hemispheres.

MATERIALS and METHODS

Animals

Homozygous male DCX-Luc mice (n = 72) with C57BL/6 albino background (B6(Cg)-Tyrc-2J/J) were used for all experiments. These mice include the human DCX promoter which controls the wildtype firefly luciferase, and were characterized in detail earlier (Couillard-Despres et al., 2008). Mice were of three different age groups: 2 months ("2M", n=28), 6 months ("6M", n=29) and 12 months ("12M", n=27). All animal experiments comply with the ARRIVE guidelines (Kilkenny et al., 2010) and were conducted according to the national, German and Austrian, guidelines in accordance with the European Council Directive 2010/63/EU, and were approved by the local authorities (Landesamt für Natur, Umwelt und Verbraucherschutz North Rhine-Westphalia, reference number 84-02.04.2011.A123; Salzburger Landesregierung, Abteilung 9 für Gesundheit und Sport 20901-TVG/84). Animals were housed in individually ventilated cages under 12 h light/12 h darkness cycle with access to water and food ad libitum.

MCAO model

Focal cerebral ischemia was induced using the filament model as described by Bahmani et al. (Adamczak et al., 2014; Bahmani et al., 2011). Briefly, mice were anesthetized with 1-2% isoflurane in an O_2/ N_2O (30:70%) gas mixture and received a subcutaneous (s.c.) injection of 4 mg/kg Carprofen (Rimadyl) for analgesia. Silicon rubber-coated filaments (Doccol Corporation, Sharon, MA USA) with tip diameters of 170 µm, 190 µm, and 200 µm were used for the 2M, 6M and 12M group, respectively, to block the blood flow to the middle cerebral artery (MCA). Animals were allowed to recover during the 30 min occlusion in a temperature stable box (MediHeat, Peco Services Ltd., Brough, UK) and subsequently re-anesthetized to initiate reperfusion by filament removal. The common carotid artery (CCA) was permanently ligated. Sham animals received only a permanent ligation of the CCA. Following these surgical interventions, body weight was monitored daily for 1 week after stroke.

Experimental design and group allocation

The study consisted of two groups: the BLI group for the longitudinal neurogenesis time profile generation, and a separate histology group for the immunohistochemical analysis at the time point of maximal neurogenic response after stroke (determined in the first group to be at day 4 post stroke).

Animals in the BLI group received a pre-MCAO measurement for bioluminescence imaging (BLI) and MRI. This allows the evaluation of the pre-stroke distribution of DCX+ neuronal precursor cells (NPCs) via bioluminescence imaging (BLI) signal, as well as the detection of any abnormalities in brain anatomy via MRI. The number of DCX+ cells is a valid measure of neurogenesis as we reported previously (Couillard-Despres et al., 2005). On day 0, animals underwent surgery (MCAO n=54, SHAM n=18) as described above. Animals were measured by MRI for the evaluation of the stroke lesion at 2, 7, and 21 days after surgery. Bioluminescence imaging for NPC distribution was performed at 4, 7, 14, and 21 days after stroke. Animals were then sacrificed for immunohistological evaluation of the brain at day 21 after stroke.

Based on the MRI measurement at day 2 after surgery, animals were included (n=33) or excluded (n=39) from the study. For group homogeneity, only animals with cortico-striatal ischemic lesion were included in the study. Exclusion criteria were: i) ischemic lesion covering only striatum without cortical involvement, ii) stroke involving the hippocampus, iii) no successful stroke induction on T2-weighted MRI at 48 hours, iv) death, v) lesion after sham surgery, or vi) anatomic abnormalities before stroke induction detected on T2-weighted MRI (Supplementary Fig. 1). Finally, group sizes were as follows: “2M” MCAO n=5, “2M” SHAM n=5, “6M” MCAO n=6, “6M” SHAM n=4, “12M” MCAO n=9, “12M” SHAM n=4 (Supplementary Fig. 1). It should be noted that death after MCAO or sham surgery was not affected by aging (death after stroke: 2M – 1; 6M – 3; 12M – 1; death after sham surgery: 2M – 0; 6M – 1; 12M – 1).

Animals in the histology group received MCAO, as described above, and were sacrificed for histological evaluation of the brains at day 4 after MCAO, the time point determined by the BLI group to be the time point of maximal neurogenesis. For this group, mice of 2 months (MCAO n = 3, SHAM n = 3) and 12 months (MCAO n = 3, SHAM n = 3) of mixed gender were used to cover the extreme ends of the neurogenesis age dependence.

Magnetic resonance imaging (MRI)

Experiments were performed on a horizontal 11.7 Tesla Bruker BioSpec 117/16USR system (Bruker Biospin, Ettlingen, Germany) with a 16 cm horizontal bore magnet. RF transmission was achieved with a quadrature resonator (Bruker) and the signal was detected using a mouse quadrature surface coil (Bruker). Animals were anesthetized with 2% isoflurane in O_2/N_2O (30/70 %) and mounted in an animal holder. Anesthesia was monitored with a pressure sensitive pad placed under the thorax, and body temperature was maintained at 37 °C with an in-house feedback-controlled system, together with DASYLab (Measurement Computing, Norton, USA).

Anatomical 1H MRI was performed with a turbo spin echo sequence. In order to maintain slice orientation throughout the experiments, whole brain turbo spin echo sequence (TR/TE = 4500 ms / 33 ms, 25 slices, slice thickness 0.6 mm, FOV 2 x 2 cm^2, matrix 196 x 196, resolution 102 x 102 μm^2) was adjusted on a sagittal plane (same parameters, 1 slice). A multi slice multi echo (MSME) sequence (TR/TE = 4500 ms /10 ms, 16 echoes, 10 or 12 slices, slice thickness 0.6 mm, FOV 2 x 2 cm^2, matrix 196 x 196, resolution 102 x 102 μm^2) was measured for T2 evaluation and visualization of lesion location. T2 maps were calculated with IDL software (Exelis Visual Information Solution, Boulder, CO, USA). Horizontal images were acquired with a FLASH sequence (TR/TE = 90 ms / 10 ms, 3 slices, slice thickness 0.7 mm, FOV 2 x 2 cm^2, matrix 256 x 192, resolution 78 x 104 μm^2) for visualisation of the lesion in the horizontal plane for the same perspective as used for bioluminescence images. The coronal anatomical turbo spin echo images of the 2M group (pre stroke n=17) were coregistered with FSL (FMRIB Software Library; Oxford, UK) FLIRT (12 degrees of freedom) and data was averaged to create a template brain.

For all subsequent imaging sessions the turbo spin echo sequence was coregistered to the template with the same coregistration procedure. The coregistration matrices were then used to realign the T2 maps. For reliable and objective discrimination of the ischemic territory a T2 threshold above normal was determined. For this purpose, the average T2 value of the cortex from the intact hemisphere across all animals of all age groups was calculated. The threshold was set at T2 values elevated by 10% or more above this average value. Further, a mask was created for every age group and every measurement time point to exclude the ventricles from the lesion on the T2 maps. From the coregistered T2 maps and the ischemic T2 threshold, stroke incidence maps were then created and stroke volumes were calculated.

Bioluminescence imaging

One day prior to every bioluminescence imaging session, mice were anesthetized in 2% isoflurane and the fur on the head was removed using depilatory cream to allow better photon penetration.

To determine the age dependent decrease in photon emission of healthy animals, mice received a 150 mg/kg D-luciferin sodium salt (Synchem, Felsberg, Germany) injection i.p. directly before anesthesia with 2% isoflurane. Subsequently, photon emission was measured from consecutive measurements of auto-exposure time performed every minute for 1 hour and the area under curve (AUC) was determined. Photon emission was recorded with the IVIS SPECTRUM (Perkin-Elmer, Waltham, MA, USA).

Mice, submitted to stroke, received 300 mg/kg D-luciferin sodium salt (Synchem, Felsberg, Germany) i.p. and were subsequently anesthetized in 2% isoflurane. Photon emission was captured using the IVIS SPECTRUM CT (Perkin-Elmer, Waltham, MA, USA). The acquisition was started directly after luciferin injection. Thirty consecutive measurements of auto exposure time were performed every minute in order to capture the kinetics of luciferin distribution during the first 30 min post injection. Maximum photon emission (PE_{max}) was extracted from the kinetic curves. Photon emission was analyzed for the left and right hemisphere by manually placed rectangle region of interests (ROIs) of fixed size. For analysis of the longitudinal study after stroke induction, the values of ischemic ROIs (right hemisphere) were normalized to those of the intact (left) hemisphere ROIs and displayed as mean ± standard deviation. This was done to avoid fluctuation in signal strength due to variation in luciferin uptake at individual time points.

Immunohistochemistry

Animals of the BLI group were deeply anesthetized under isoflurane at 21 days after stroke induction and transcardially perfused with 20 ml ice-cold PBS followed by 20 ml 4% paraformaldehyde (PFA). Subsequently, brains were removed and post-fixed in PFA overnight at 4°C, followed by 30% sucrose cryoprotection. Brain tissue was stored at -80 °C until further processing. Brain sections of 30 µm thickness were coronally cut on the cryostat (Leica Microsystems, Wetzlar, Germany) and stored at -20 °C. Prior to immunostaining, sections were pre-incubated at room temperature in 5% normal serum and 0.25% Triton X-

100 in KPBS for 45 minutes. Goat-anti-DCX (1:50, AB 2088494, sc-8066, Santa Cruz Biotechnology, Heidelberg, Germany) was used as primary antibody and incubated overnight at 4 °C. A Cy3 donkey anti-goat antibody (1:200, AB 2339464, Jackson Immuno Research Europe Ltd., UK) was applied for 2h at room temperature. Hoechst 33342 (1:1,000 Invitrogen, Carlsbad, USA) was added during final incubation with secondary antibodies for nuclear staining. Slides were coverslipped with mounting medium (Entellan, Merck, Darmstadt, Germany).

Animals of the histology group were deeply anaesthetized at day 4 after stroke induction and were transcardially perfused with 0.9% NaCl for 5 min, followed by 0.1 M phosphate buffered 4% paraformaldehyde pH 7.4 for 10 min. Brains were dissected and post-fixed in the formaldehyde solution overnight at 4°C and then transferred in 0.1 M phosphate buffered 30% sucrose solution pH 7.4 at 4°C for at least 48 h. Brains were cryosectioned in 40 µm coronal sections and were stored at -20°C until further processing.

For immunohistological analysis sections were washed with PBS + 0.1 %Tween 20 (Sigma-Aldrich), and blocked with 1 % BSA (Sigma-Aldrich), 0.2 %Fish Skin Gelatine (Sigma-Aldrich) and 0.1 % Tween 20 (Sigma). Sections were incubated overnight at 4° C in the blocking solution containing the following antibody dilution: guinea-pig anti-GFAP (Progen, 1:500) and rabbit anti-DCX (Cell Signaling Technology, 1:300). The following secondary antibody dilution was used: donkey anti-rabbit Alexa 488 (Invitrogen, 1:1000) and donkey anti-guinea-pig Alexa 568 (Invitrogen, 1:1000), containing 4’6-diamidino-2-phenylindole (DAPI, Sigma-Aldrich, 0.5 µg/ml) at room temperature for 4 hours. Finally, sections were mounted with DAKO fluorescence mounting medium (Agilent Technologies). Micrographs were acquired from a maximal intensity projection of the whole section thickness using a Zeiss LSM700.

Statistical analysis

Statistical analysis was performed with SPSS version 15 (IBM SPSS statistics, Ehningen, Germany). Age-dependent changes of photon emission and T2 in healthy animals was tested using a one way ANOVA with Bonferroni corrected post-hoc comparisons. To test for differences in lesion volume between the three age groups a one way ANOVA was also used.

Longitudinal *in vivo* BLI data was tested for significant changes using a repeated measures analysis of variance (RM-ANOVA) with Bonferroni corrected post-hoc comparisons.

RESULTS

Non-invasive imaging detects age-related changes in physiological neurogenesis

The bioluminescence signal of the DCX-luc transgenic mouse provides direct quantitative *in vivo* information on the level of neurogenesis which correlates with the abundance of DCX-expressing neuroblasts. We measured healthy mice at various ages between 2 and 21 months of age and found a strong decrease of basal neurogenesis during the first 9 months (Fig. 1A). From 2 to 9 months the bioluminescence signal dropped by approximately 50% and thereafter, only slightly further decreased.

To investigate the neurogenic response to ischemic stroke, we therefore chose three age groups to cover this age span with the most severe drop in neurogenesis: 2 months for young animals, 6 months for young adults, and 12 months for aged animals with low neurogenesis regime. Bioluminescence signal intensity showed, in agreement with the life time coverage between 2 and 21 months (Fig. 1A), a statistically significant drop over time (Fig. 1B; $F(2.30)=28.998$ $p<0.001$) resulting in approximately 50% signal intensity at 12 months relative to the 2 months value ($p<0.0001$).

Ischemic lesion severity across ages

In order to determine stroke lesion size on quantitative T2 MRI maps, we determined stability of T2 values in healthy cortex and striatum for the same mice at 2, 6, and 12 months (Fig. 1C). Both, striatum and cortex showed significant reduction in T2 over time (striatum: $F(2.15)=28.565$ $p<0.001$, cortex: $F(2.15)=4,670$ $p=0.024$) but with significant posthoc analysis only in the striatum ($p<0.0001$). This small, but continuous decrease in T2 value is explained by reduction of the extracellular space and myelination, two processes being shown to continue at least till 6 months of age (Hammelrath et al., 2016; Mengler et al., 2014). As the T2 values of the cortex showed no clear age dependence and were slightly higher than for striatum, the average T2 of cortex across all age groups at $T2_{ctx}$ = 30.6 ms was used to

determine a conservative low threshold of $T2_{ctx}$+10%($T2_{ctx}$) = 33.7ms for the discrimination between normal tissue and ischemic tissue with elevated T2 values (cf. Materials and Methods section).

Using this threshold of 33.7 ms while excluding all ventricular spaces, the ischemic lesion size at 48h after stroke induction was determined. Average stroke volume did not differ significantly between 2 months (24 ± 12 mm^3), 6 months (40 ± 20 mm^3), and 12 months (28 ± 10mm^3) old animals. The spread of the lesion across cortex and striatum is shown in lesion incidence maps for the three age groups, clearly demonstrating well comparable lesion location and extent (Fig. 2).

Neurogenesis response to stroke

We acquired longitudinal BLI and MRI from mice of all three ages (2M, 6M, and 12M) in order to quantitatively assess intra- as well as inter-individual differences in stroke lesion and neurogenic response. Figure 3 shows the BLI pattern for representative animals of each age group, being symmetric for both hemispheres in the healthy mice. In the healthy condition, one can already discern the drop in photon emission during aging, representing the decrease in basal neurogenesis during the aging process (cf. Fig. 1A, B).

Four days after stroke induction, measurement of the kinetic curve of the photon emission revealed that the overall bioluminescence signal intensity over the ischemic hemisphere increases above that of the healthy contralateral hemisphere (Supplementary Fig. 2). This specific signal increase is reflected in the BLI data (Fig. 3) as a clear shift of the center of gravity of the neurogenesis to the ischemic hemisphere as compared to the symmetric BLI situation before stroke. This shift of the BLI intensity center colocalized well with the location of the ischemic territory depicted on the corresponding horizontal MRI images. This pattern of BLI increase and shift is independent of age group studied (Fig. 3) and indicates that all age groups are capable to react to stroke with increased neurogenesis, predominantly occurring in the ipsilateral hemisphere. At 3 weeks after MCAO, the intensity of DCX-associated BLI cells has returned almost to pre-stroke values, and the lower basal neurogenesis at the older age groups becomes visible again. In comparison, sham animals showed neither change in signal intensity over time nor a deviation from a clearly symmetric signal intensity distribution across the two hemispheres (Fig. 4).

To follow the neurogenesis response to stroke induction quantitatively over time, the bioluminescence signal over the right (ischemic) hemisphere was normalized to the value over the left (contralateral, healthy) hemisphere. In sham animals, the signal intensity from left and right hemisphere was equal, remained stable during repetitive recordings over several weeks, and was independent of age group (Fig. 4 left column). Stroke induction resulted in an increase of photon emission in the ischemic hemisphere, being similar in the different age groups. There was a rapid BLI increase reaching its maximum at 4 days, followed by a slow and continuous decline over the next two weeks when BLI relative intensity returned to pre-stroke values again (Fig. 4, right column). This temporal profile of the bioluminescence pattern over time was observed for all three age groups. The maximal values at 4 days post stroke were for all age groups statistically significantly different from both, the pre-stroke values and the final values at three weeks after stroke induction. At the maximum on day 4, 2M old animals had a bioluminescence increase of 28 ± 10 %, in 6M old animals it was 19 ± 14 %, and 31 ± 11 % in 12M old mice. Statistical analysis revealed no significant changes between age groups.

Separate analysis of hemispheres for neurogenesis after stroke

In a next step, we analyzed the behavior of the two hemispheres independently of each other using the absolute BLI values. For the older age groups, we found a significant reduction in basal neurogenesis at the pre-stroke time point, being absolutely equal on both hemispheres (Fig. 5 A, B). Ipsilateral to the stroke (Fig. 5A), a clear increase in photon emission (at day 4 post stroke) was observed with a pronounced trend towards stronger increase in older animals. While the neurogenic response relative to pre-stroke basal neurogenesis was 28% for the 2M old animals, it increased by 68% for 6M old animals and by even 90% for the 12M old mice. This means that the weaker basal neurogenesis in older animals has been compensated by a much stronger increase in DCX-associated signal, stimulated by the ischemic event. In consequence, this elevated neurogenic response with increasing age may compensate for the lower basal neurogenesis and provide the system with a comparable amount of newborn cells which can be recruited to the stroke core to support recovery.

Contralateral to the stroke, a significant response to the stroke was also detected, but limited to the older animals (6M and 12M; Fig. 5B). The neurogenic increase on the healthy

hemisphere relative to the pre-stroke situation was 42% at 6M (p=0.018) and even 46% at 12M (p=0.025). This demonstrates that normalization to the contralateral side, as was done for the data presentation in Fig. 4, actually underestimated the actual neurogenic response to stroke in 6M and 12M age groups, while still documenting the true response strength for the young animals at 2 months of age. When using the two enhancement factors of 42% (6M) and 46% (12M) of the contralateral hemisphere as correction factors for the increase values found in Fig. 4, one ends up again with the absolute ipsilateral neurogenesis enhancement of 28% (2M), 70% (6M) and 91% (12M) in full agreement with the values directly extracted from the ipsilateral hemisphere (Fig. 5A). In comparison, the sham animals showed a bioluminescence signal of both hemispheres that remained equal to the pre-stroke values (Supplementary Fig. 3), again for all age groups.

The findings from the separate analysis of the two hemispheres (Fig. 5) were confirmed when the data of each hemisphere (ipsi- and contralateral) were normalized to the data of the sham group of the corresponding age. Again, the increase of neurogenesis on the contralateral hemisphere became substantially pronounced with increasing age while young animals (2M) did not show such a clear increase on the contralateral side.

Immunohistochemical confirmation of neurogenesis after stroke

Immunohistological staining of brain slices for GFAP-positive astrocytes and DCX-expressing neuroblasts confirmed astrogliosis on the ischemic hemisphere and existence of neuroblasts surrounding both lateral ventricles at three weeks post stroke (Fig. 6A). The age-independent neurogenic response seen in the BLI data is reflected by the persistent DCX staining for all age groups on the ipsi- and contralateral SVZ. In contrast, GFAP/DCX-staining of sham animals clearly indicates the absence of astrogliosis in all age groups and the age-dependent decrease in DCX-expressing neuroblasts (Fig. 6B). These sections reveal the situation at 3 weeks post stroke, when the neurogenic response to stroke had already subsided to near pre-stroke values in all age groups. In accordance to our *in vivo* results, no imbalance between ischemic and intact SVZ was visible in the DCX population within the SVZ at this time. However, only in 2 months old mice, lateral migration of SVZ-neuroblasts through the corpus callosum and the striatum was detected.

Four days post-ischemia, i.e. the time point of strongest neurogenic response, the massive migration of the DCX-expressing neuroblasts towards the lesioned striatum could be detected in the 2 months old as well as the 12 month-old mice (Fig 7). Although the SVZ appeared

broader in the ischemic as compared to sham-operated mice, emigration of DCX-expressing neuroblasts into the striatum was not only induced in the ipsilateral hemisphere (Fig.7 I-J, M-N). Also, at both ages, reactive astrogliosis was much more pronounced in the ipsilateral than in the contralateral hemisphere. The density of DCX-expressing neuroblasts in the dentate gyrus dramatically dropped when the ischemic lesion was close (Fig. 7K), or remained stable with increased distance to the lesion (Fig. L). Similarly, the contralateral dentate gyrus remained unaffected (Fig. 7G-H, O-P). Considering the small number of neuroblasts in the dentate gyrus, in comparison to the SVZ, and their apparent absence of response to lesion, the fluctuation of neurogenesis measured longitudinally with BLI after stroke arises primarily from the SVZ.

DISCUSSION

We have studied the development of neurogenesis at the level of doublecortin-expressing neuroblasts in response to stroke. As stroke is a disease prevalent in elderly people, we have first characterized the age-dependent decrease of basal neurogenesis in our model for neuroblast detection with the DCX-driven luciferase bioluminescence signal. Based on this age-dependence, three age groups were defined representing young animals (2M), early adults (6M), and a third group at 12 months where the basal neurogenesis was closely the same as for old animals at 21 months (Fig. 1). In these three age groups, we have studied the neurogenic response to stroke during the acute period of the first three weeks after stroke onset. To the best of our knowledge, this is the first study assessing the *in vivo* temporal profile of neurogenesis after stroke as a function of age using non-invasive imaging. We have shown that neurogenesis at the level of DCX^+ neuroblasts has its maximum at four days post stroke, independent of age. Older brains express an increased sensitivity to stroke, i.e. enhancing the upregulation of neurogenesis even further to compensate almost completely for the substantially lower basal neurogenesis in older brains. An interesting new observation consists in the enhanced neurogenic response to stroke in the SVZ of the healthy hemisphere of older animals, not found for young mice.

Methodological considerations

Bioluminescence imaging quantification is challenging, requiring a standardized protocol for the data recording, and optimized for maximal bioluminescence detection sensitivity in the brain (Aswendt et al., 2013; Mezzanotte et al., 2013). Substrate injection i.p. may result in slight variations of total photon flux due to individual difference in luciferin absorption into the vascular system. To minimize such experimental error between each session, we used the contralateral hemisphere as internal control for every measurement. Normalization to the contralateral intact hemisphere excludes the injection/absorption-induced variation in photon flux and allows observation of robust individual time curves (Fig. 4). However, this methodological approach is no longer valid if the normalizing site itself is not stable, as in our case. Here, in our experimental condition, two factors modulated the neurogenesis level of the healthy hemisphere: the age dependent decrease of basal neurogenesis and the stroke induced enhancement of neurogenesis on the healthy SVZ in older animals. In such cases, absolute photon emission analysis is required and, as demonstrated in the present investigation, is sound to use for groups of animals. The procedure provides reliable absolute quantification of DCX-reporter expression over time (Fig. 5).

Quantification of bioluminescence imaging data is achieved by the AUC as well as the PEmax approach (Aswendt et al., 2013), which qualifies better for studies on ischemic animals due to shorter acquisition time required for robust data. The equivalence of both approaches is proven by data presented in Figure 1 A and B, showing the same magnitude in age-dependent decline in neurogenesis. We combined BLI with sequential MRI to monitor the stroke development and correlate the ischemic territory to the mouse age and neurogenic response. Superior to invasive studies, our noninvasive approach highlights the inter-individual time-profile of neuroblast accumulation upon stroke induction and uses pre-stroke data as intra-individual baseline. As shown in our previous study characterizing the DCX-Luc mice, the spatial resolution of BLI allows here only to identify the numerous DCX+ cells near the ventricles and in the olfactory bulb, while the few hippocampal neuroblasts cannot be resolved (Couillard-Despres et al., 2008). Therefore, our analysis and data interpretation is limited to the neurogenic response originating from the SVZ, while neglecting hippocampal involvement. BLI with improved lateral and most importantly depth resolution could help in future studies to make this regional distinction.

Noninvasive imaging detects age-related changes in neurogenesis

We have demonstrated the age-dependent neurogenesis modulation with a noninvasive imaging approach, providing easy quantification of the abundance of DCX-expression compared to classical, time consuming histological evaluations. Moreover, our imaging based approach allows repetitive assessments over time to compile temporal profiles. We have observed that the major decline in adult neurogenesis of mice appeared already within the first year with a drop in neurogenesis down to almost 50% of young adult (2 months old). Our results, on the basis of DCX-expressing neuroblasts, are in agreement with several studies on rats and mice focusing on various stages of neurogenesis from NSC (Shook et al., 2012) to DCX^+ neuroblasts (Luo et al., 2006), as summarized in a recent review by Hamilton et al. (Hamilton et al., 2013). Several factors have been discussed as cause for this age-dependent decrease in neurogenesis (Hamilton et al., 2013; Molofsky et al., 2006). Recent studies indicate that the age-related decline is not only dependent on an intrinsic change of the precursors, but is also sensitive to changes in the neurogenic microenvironment (Villeda and Wyss-Coray, 2013), raising the opportunity to profit from endogenous neurogenesis for therapeutic application even in elderly people.

Ischemic lesion severity across ages

Brain aging occurs not only in the neurogenic niches, but affects the whole brain. Reduction of the extracellular matrix and increase in myelination can be observed across the brain and can be detected as changes of T2 values (Mengler et al., 2014). We found changes in T2 in the striatum and the cortex of healthy aging mice (Hammelrath et al., 2016) consistent with observations in aging rats (Mengler et al., 2014). These changes already occur in the first year after birth and support that cardinal aspects of aging take place between the age groups of 2, 6, and 12 months, as selected in the present study. Models of experimental stroke in old, versus young, animals resemble the situation in human patients and show stronger reduction of neurological function as well as higher vulnerability for acute neurodegeneration (Onyszchuk et al., 2008; Tokutomi et al., 2008; Yager et al., 2006). Here, we found that the standardized model of 30 min MCA occlusion in the mouse leads to stroke lesion volumes not significantly different between the age groups. This is in good agreement with previous observations in rats (Darsalia et al., 2005; Popa-Wagner et al., 2007). It has been suggested

that not the infarct size, but the timing of neuronal loss is accelerated in aged mice (Popa-Wagner et al., 2011)

Neurogenic response after stroke

The neurogenic response to stroke at the level of DCX-expressing neuroblasts was found to have its maximum at about 4 days after stroke onset. This maximal response time was independent of age of the animals. This is the first study, to the best of our knowledge, reporting the temporal profile of neurogenic neuroblast response to stroke, using noninvasive molecular imaging. We have followed the enhancement of SVZ neurogenesis over three weeks following stroke and across the age from young to old mice. Interestingly enough, most studies addressing the neurogenic increase after stroke have been performed in rats (Darsalia et al., 2005; Jin et al., 2004; Sato et al., 2001; Takasawa et al., 2002; Tang et al., 2014) and have studied only discrete time points after stroke. Jin et al. observed a higher increase of $BrdU^+$ cells at 24 hours after stroke in 3 months young compared to 24 months old animals (Jin et al., 2004). These authors did not characterize the cells further and compared the increase on the ischemic hemisphere only to sham animals but not to contralateral hemisphere. Takasawa and colleagues reported a maximal increase of $BrdU^+$ cells in the SVZ of 2 months young rats at day 7 (Takasawa et al., 2002). Sato et al. described a maximal enhancement of PSA-$NCAM^+$ cells at day 1 or day 3 post stroke for 3 months young and old rats, respectively (Sato et al., 2001).

In a recent study by Tang et al. (Tang et al., 2014), the number of $DCX^+/BrdU^+$ cells was found to be half as high for 24 months old animals at 2 weeks after stroke, when compared to 3 months old rats. This is in complete agreement with our present results because at 2 weeks after stroke onset the maximal neurogenic response has already levelled off again and returned close to baseline, thus reflecting only the difference in basal neurogenesis for the two ages. Darsalia and colleagues studied neurogenesis 7 weeks after stroke, when BrdU was applied during the first two weeks (Darsalia et al., 2005). Thus the results integrate the whole neurogenic upregulation during these two weeks, making it impossible to discriminate a maximal response time point. These authors report equivalent numbers of $DCX^+/BrdU^+$ cells at 7 weeks for 3 and 15 months old animals. This is in agreement with our own results as the two-week long integration should reflect the closely similar time curve with similar enhancement maxima at 4 days for young and old animals in our study on mice. Darsalia et al. also reported a lower number of $Ki67^+$ cells in aged animals at 7 weeks, which agrees with

our findings that at this late time point after stroke, neurogenesis is already back to basal level, independent of stroke, i.e. reflecting simply the age dependent basal neurogenesis (Darsalia et al., 2005).

Only one study previously assessed the neurogenesis in mice in relation to stroke (Vandeputte et al., 2014). These authors have described a maximum neurogenic response at 14 days after stroke induction. This is one week later than in Takasawa's (Takasawa et al., 2002) and our own present findings and may be due to several differences in experimental protocol. Vandeputte and colleagues induced luciferase expression by lentiviral injection in the SVZ, only one week before stroke induction. Thus, it cannot be excluded that the full viral expression takes longer than one week, and hence the bioluminescent signal intensity lags behind the stroke evolution and the neurogenic response. Further, those authors had used the photothrombotic stroke model which limits the lesion to the cortical region and has a different pathophysiological characterization than the clinically more relevant MCAO model. This might result in weaker (and even delayed) neurogenesis upregulation.

Following normalization of the neurogenic response based on the contralateral side, the maximum intensity at 4 days post stroke had a similar magnitude across the age groups. However, taking the progressive reduction of basal neurogenesis with increasing age into account, aged animals respond to the ischemic lesion process with substantially larger increase in DCX-cell production in the subventricular zone. The absolute signal intensity emanating from DCX^+ cells at day 4 after stroke was only slightly, but not significantly different between the 2, 6, and 12 months old mice. Considering that the neurogenic increase started from the much lower basal level, the effectively similar enhanced level suggests a profoundly enhanced sensitivity of older brains to their insults, and reacting with compensatory mechanisms to the lower basal neurogenesis in the aged brain. This subsequently results in the generation of DCX^+ neural progenitor cells almost up to the level of young animals.

Our observations in mice and previous ones obtained in rats (Darsalia et al., 2005) support the hypothesis, that it is the microenvironment of the neurogenic niche that influences the intensity of the response to stroke, rather than cell intrinsic factors (Hamilton et al., 2013; Molofsky et al., 2006; Villeda and Wyss-Coray, 2013). Additional support comes from *in vitro* comparisons of explanted neural stem cells from young versus old mice, which showed

same survival, migration and differentiation capacity (Ahlenius et al., 2009). In this context it is interesting to note that intensive interactions between NSCs and immune cells have recently been discussed (Kokaia et al., 2012), as they share many cytokines, chemokines and growth factors. Hu and colleagues (Hu et al., 2012) reported that during the first week after stroke the neuroprotective, beneficial polarization (M2) state of the inflammatory cells dominates. Notably, the anti-inflammatory M2 promoting cytokine IL-10 peaks at 5-6 days post stroke, which may have a direct effect on progenitor cell upregulation, as has been recently reported for basal neurogenesis (Pereira et al., 2015). Although there is no direct evidence yet, it is tempting to consider that our observation of maximal neurogenesis at day 4 coincides with the M2 polarization state of inflammatory monocytes and microglia.

Interestingly, we have found a strong contralateral activation of the neurogenic response to stroke in adult and old, but not young adult animals. Most previous studies have focused only on the neurogenic change in the ischemic hemisphere, ignoring any potential stroke induced alterations on the healthy hemisphere (Tang et al., 2014) or have compared their findings only to sham animals (Jin et al., 2004; Sato et al., 2001), i.e. to normal basal neurogenesis condition. Darsalia et al. had integrated the neurogenic enhancement over the first two weeks with their BrdU labeling protocol (Darsalia et al., 2005), so that the small, but significant increase on the contralateral side would most likely be lost in the broad integration. Only in Takasawa's report on the hippocampal neurogenesis after stroke, a slightly increased number of $BrdU^+$ cells after the first day was reported without any further characterization of cell type (Takasawa et al., 2002). Here, we have demonstrated for the first time a statistically significant increase in neurogenesis on the contralateral hemisphere for the 6 months and 12 months old mice but not for the young animals (Fig. 5B). This enhanced sensitivity parallels the higher sensitivity of neurogenic response of the ischemic hemisphere of older animals, obviously a compensation for the age dependent decrease in basal neurogenesis. We see this as further indication that neurogenesis is upregulated to a level considered necessary to contribute to endogenous regenerative processes after cerebral lesions at all ages. Future studies will be necessary to decipher the potential of these contralaterally generated neuroblasts to migrate, differentiate and contribute to functional recovery after stroke.

CONCLUSIONS

Despite age-dependent decrease of basal level of DCX^+ neuroblasts, neurogenesis upregulation during the first week after stroke is further enhanced with increasing age to reach elevated levels of neuroblasts at middle-age (6M) fully equivalent to those of young (2M) animals. Old animals (12M) still reach almost the same level as young mice. This age dependent enhancement is seen as increasing sensitivity to the cerebral lesion to compensate for lower basal levels. Furthermore, the lesion-induced neurogenic response led to an additional increase of neurogenesis on the contralateral healthy hemisphere in the groups of 6 and 12 months of age. These observations reveal that the endogenous neural stem cells retain their potential and can be re-awaken to action by correct cues. Thus, our findings emphasize the therapeutic relevance and potential of endogenous neurogenesis in stroke recovery for elderly people.

FIGURE LEGENDS

Figure 1 Changes in neurogenesis and T2 values during aging of healthy mice

A) *In vivo* bioluminescence imaging of homozygous DCX-luc mice shows a significant age-dependent reduction (linear regression with p=0.185) in basal neurogenesis in the brain. Data plotted as area under curve (AUC) referring to total photon counts. **B)** Measurement and analysis method were adjusted to be in line with the later stroke study. Using the maximal photon emission (PEmax) the bioluminescence signal of DCX-luc mice, included into the stroke study, reveals also a significant gradual reduction of basal neurogenesis from 2 to 12 months. **C** The process of aging can be visualized by changes of the T2 values in quantitative MRI measurements. Significant reduction of T2 was detected in striatum and cortex during aging. * $p<0.05$, ** $p<0.01$, *** $p<0.001$

Figure 2 Incidence maps for stroke location and lesion volume of different age groups

Incidence maps are displayed on corresponding anatomical MR images. Color bars indicate the number of animals of each group with pixels considered as stroke-affected area based on T2 mapping. Lesions included striatum and cortex in all age groups. Stroke size was independent of age.

Figure 3 Magnetic resonance imaging and bioluminescence of neurogenesis after stroke

Representative horizontal FLASH MR images are displayed next to the corresponding bioluminescence images of all age groups and time points (pre stroke, 4 days and 3 weeks after stroke). Pre-stroke bioluminescence signals were equal in left and right hemisphere in all groups of age, but absolute photon emission, thus basal neurogenesis, decreased from 2 to 12 months. Four days post stroke a strong increase in photon emission was detected in the ischemic territory which directly correlates with the lesion detected with horizontal T2 weighted MRI images (hyperintense region). Three weeks after stroke, increased bioluminescence signals in the stroke area vanished.

Figure 4 Quantification of stroke induced neurogenesis in different age groups

Blue curves represent individual animals. Mean of the group is displayed as red thick overlaying curve. Values were gained by extracting PEmax for ischemic and intact hemisphere. Subsequently, the ischemic PEmax was normalized to the intact PEmax in order

to exclude inter-measurement variability. Sham animals do not show increased bioluminescence signals of the sham side relative to the intact hemisphere. MCAO animals show an increase of 28% (2 months old, **A**), 68% (6 months old, **B**), and 90% (12 months old, **C**) relative to the intact hemisphere with peak values during the first week after MCAO. * $p<0.05$, ** $p<0.01$, *** $p<0.001$

Figure 5 Quantification of absolute photon emission

The graphs represent maximal photon emission (PEmax) from pre-stroke (black bars) and post stroke (blue bars) per age group with 2 months pre-stroke set to 100 %.

A The ischemic hemisphere shows significant PEmax increase only for 6 and 12 months old mice but significant PEmax decrease with age only for pre-stroke values. Interestingly, a difference in magnitude between ages is statistically not detectable. **B** Also the contralateral hemisphere data reflects the reduction of basal neurogenesis with proceeding age. Post stroke values (4 days post stroke) show a neurogenic response to stroke even in the intact hemisphere. However, only at 6 and 12 months neurogenesis in the intact hemisphere is significantly upregulated. * $p<0.05$, ** $p<0.01$, *** $p<0.001$

Figure 6 Immunohistochemistry for doublecortin at 3 weeks after stroke

Whole brain slice images with subsequent magnified images are shown for 2, 6 and 12 months of stroke (A) and sham (B) mice. A) GFAP-reactivity (green) on the ipsilesional hemisphere indicates astrogliosis around the ischemic lesion (scale bar 500 um). Bilateral SVZ DCX-positive cells encircle the SVZ bilaterally in all age groups (middle row, scale bar 250 um). Zoomed-in images from the dorsal part of the ventricle at the border of the corpus callosum (1, 2) and towards the striatum (3, 4) highlight the persistent production of DCX-positive neuroblasts among all age groups (scale bar 25 um). B) Age-dependent reduction in basal neurogenesis is confirmed by an increase of discontinuity of DCX staining in the SVZ. Three weeks post stroke neurogenesis is back to baseline levels in all groups of age.

Figure 7 Immunohistochemistry for doublecortin at 4 days after stroke

Representative coronal sections of a (A) 2 months old sham mouse, (B) 2 months old MCAO mouse, (C) 12 months old sham mouse and (D) 12 months old MCAO mouse. Neuroblasts are detected using an anti-DCX antibody (green) and astrocytes using an anti-GFAP (red), cell nuclei are labeled with DAPI (blue). The SVZ of (E) 2 months old and (F) 12 months old sham mice revealed numerous neuroblasts. Four days following ischemia, numerous

neuroblasts from the ipsilateral SVZ migrated towards the lesioned striatum in the (I) 2 months old and (J) 12 months old mice, whereas neuroblasts remained within the SVZ on the contralateral side both in the (M) 2 months old and the (N) 12 months old mice. As expected, the dentate gyrus of sham mice contained higher number of neuroblasts at (G) 2 months, as compared to (H) 12 months of age. Following ischemia, the ipsilateral dentate gyrus proximal to the lesion had only few neuroblasts remaining e.g. (K) 2 months of age, whereas more distal region remained unaffected e.g. (L) 12 months of age. The contralateral dentate gyrus presented an abundance of neuroblasts following ischemia similar to the sham mice at (O) 2 months and (P) 12 months of age. Scale bars (N) 100 µm for E, F, I, J, M, N and (P) 25 µm for G, H, K, L, O, P.

ACKNOWLEDGEMENTS

We thank Tracy D. Farr who had contributed to pilot experiments in an early phase of the study, and Lara Bieler and Pia Zaunmair for microscopy support.

FUNDING

This work was financially supported by grants from the EU-FP7 programs TargetBraIn (HEALTH-F2-2012-279017) and BrainPath (PIAPP-GA-2013-612360) and by a grant from the German Research Foundation DFG (AS-464/1-1). In addition, this work received funding from the European Union's Seventh Framework Program (FP7/2007-2013) under grant agreement n° HEALTH-F2-2011-278850 (INMiND) and n° HEALTH-F2-2011-279288 (IDEA).

REFERENCES

Adamczak, J., Schneider, G., Nelles, M., Que, I., Suidgeest, E., Van der Weerd, L., Löwik, C., Hoehn, M., 2014. In vivo bioluminescence imaging of vascular remodeling after stroke. Frontiers in Cellular Neuroscience 8, article 274.

Ahlenius, H., Visan, V., Kokaia, M., Lindvall, O., Kokaia, Z., 2009. Neural stem and progenitor cells retain their potential for proliferation and differentiation into functional neurons despite lower number in aged brain. J Neurosci 29, 4408-4419.

Aswendt, M., Adamczak, J., Couillard-Déspres, S., Hoehn, M., 2013. Boosting bioluminescence neurimaging: an optimized protocol for brain studies. PLos One 8, e55662.

Bahmani, P., Schellenberger, E., Klohs, J., Steinbrink, J., Cordell, R., Zille, M., etc., 2011. Visualization of cell death in mice with focal cerebral ischemia using fluorsecent annexin A5, propidium iodide and TUNEL staining. Journal of Cerebral Blood Flow and Metabolism 31, 1311-1320.

Brown, J.P., Couillard-Despres, S., Cooper-Kuhn, C.M., Winkler, J., Aigner, L., Kuhn, H.G., 2003. Transient expression of doublecortin during adult neurogenesis. Journl of Comparative Neurology 467, 1-10.

Butti, E., Bacigaluppi, M., Rossi, S., Cambiaghi, M., Bari, M., Cebrian Silla, A., Brambilla, E., Musella, A., De Ceglia, R., Teneud, L., De Chiara, V., D'Adamo, P., Garcia-Verdugo, J.M., Comi, G., Muzio, L., Quattrini, A., Leocani, L., Maccarrone, M., Centonze, D., Martino, G., 2012. Subventricular zone neural progenitors protect striatal neurons from glutamatergic excitotoxicty. Brain 135, 3320-3335.

Couillard-Despres, S., Finkl, R., Winner, B., Ploetz, S., Wiedermann, D., Aigner, R., Bogdahn, U., Winkler, J., Hoehn, M., Aigner, L., 2008. In vivo optical imaging of neurogenesis: watching new neurons in the intact brain. Molecular Imaging 7, 28-34.

Couillard-Despres, S., Winner, B., Schaubeck, S., Aigner, R., Vroemen, M., Weidner, N., Bogdahn, U., Winkler, J., Kuhn, H.G., Aigner, L., 2005. Doublecortin expression levels in adult brain reflect neurogenesis. European Journal of Neuroscience 21, 1-14.

Couillard-Despres, S., Wuertinger, C., Kandasamy, M., Caioni, M., Stadler, K., Aigner, R., Bogdahn, U., Aigner, L., 2009. Ageing abolishes the effects of fluoxetine on neurogenesis. Molecular Psychiatry 14, 856-864.

Darsalia, V., Heldmann, U., Lindvall, O., Kokaia, Z., 2005. Stroke-induced neurogenesis in aged brain. Stroke 36, 1790-1795.

Enwere, E., Shingo, T., Gregg, C., Fujikawa, H., Ohta, S., Weiss, S., 2004. Aging results in reduced epidermal growth factor receptor signaling, diminished olfactory neurogenesis, and deficits in fine olfactory discrimination. J Neurosci 24, 8354-8365.

Erlandsson, A., Lin, C.H., Yu, F., Morshead, C.M., 2011. Immunosuppression promotes endogenous neural stem and progenitor cell migration and tissue regeneration after ischemic injury. Exp Neurol 230, 48-57.

Garcia-Verdugo, J.M., Doetsch, F., Wichterle, H., Lim, D.A., Alvarez-Buylla, A., 1998. Architecture and cell types of the adult subventricular zone: in search of the stem cells. J Neurobiol 36, 234-248.

Hamilton, L.K., Joppe, S.E., L, M.C., Fernandes, K.J., 2013. Aging and neurogenesis in the adult forebrain: what we have learned and where we should go from here. Eur J Neurosci 37, 1978-1986.

Hammelrath, L., Skokic, S., Khmelinskii, A., Hess, A., Van der Knaap, N., Staring, M., Lelieveldt, B.P.F., Wiedermann, D., Hoehn, M., 2016. Morphological maturation of the mouse brain: an in vivo MRI and histology investigation. NeuroImage 125, 144-152.

Hu, X., Li, P., Guo, Y., Wang, H., Leak, R.K., Chen, S.L., Gao, Y., Chen, J., 2012. Microglia/macrophage polarization dynamics reveal novel mechanisms of injury expansion after focal cerebral ischemia. Stroke 43, 3063-3070.

Jin, K., Minami, M., Xie, L., Sun, Y., Mao, X.O., Wang, Y., Simon, R.P., Greenberg, D.A., 2004. Ischemia-induced neurogenesis is preserved but reduced in the aged rodent brain. Aging Cell 3, 373-377.

Kilkenny, C., Browne, W.J., Cuthill, I.C., Emerson, M., Altman, D.G., 2010. Improving bioscience research reporting: The ARRIVE Guidelines for reporting animal research. PLoS Biology 8, e1000412.

Kokaia, Z., Martino, G., Schwartz, M., Lindvall, O., 2012. Cross-talk between neural stem cells and immune cells: the key to better brain repair? Nature Neuroscience 15, 1078-1087.

Kolb, B., Morshead, C., Gonzalez, C., Kim, M., Gregg, C., Shingo, T., Weiss, S., 2007. Growth factor-stimulated generation of new cortical tissue and functional recovery after stroke damage to the motor cortex of rats. J Cereb Blood Flow Metab 27, 983-997.

Lai, B., Mao, X.O., Xie, L., Jin, K., Greenberg, D.A., 2008. Electrophysiological neurodifferentiation of subventricular zone-derived precursor cells following stroke. Neurosci Lett 442, 305-308.

Lindvall, O., Kokaia, Z., 2011. Stem cell research in stroke: how far from the clinic? Stroke 42, 2369-2375.

Luo, J., Daniels, S.B., Lennington, J.B., Notti, R.Q., Conover, J.C., 2006. The aging neurogenic subventricular zone. Aging Cell 5, 139-152.

Mengler, L., Khmelinskii, A., Diedenhofen, M., Po, C., Staring, M., Lelieveldt, B.P., Hoehn, M., 2014. Brain maturation of the adolescent rat cortex and striatum: changes in volume and myelination. NeuroImage 84, 35-44.

Mezzanotte, L., Aswendt, M., Tennstädt, A., Hoeben, R., Hoehn, M., Löwik, C., 2013. Quantitative evaluation of luciferases in vivo bioluminescence imaging of neural stem cells. Molecular Imaging and Biology 8, 505-513.

Molofsky, A.V., Slutsky, S.G., Joseph, N.M., He, S., Pardal, R., Krishnamurty, J., Sharpless, N.E., Morrison, S.J., 2006. Increasing p16INK4a expression decreases forebrain progenitors and neurogenesis during ageing. Nature 443, 448-452.

Onyszchuk, G., He, Y.Y., Berman, N.E., Brooks, W.M., 2008. Detrimental effects of aging on outcome from traumatic brain injury: a behavioral, magnetic resonance imaging, and histological study in mice. J Neurotrauma 25, 153-171.

Pereira, L., Font-Nieves, M., Van den Haute, C., Baekelandt, V., Planas, A.M., Pozas, E., 2015. IL-10 regulates adult neurogenesis by modulating ERK and STAT3 activity. Frontiers in Cellular Neuroscience 9, article 57.

Popa-Wagner, A., Badan, I., Walker, L., Groppa, S., Patrana, N., Kessler, C., 2007. Accelerated infarct development, cytogenesis and apoptosis following transient cerebral ischemia in aged rats. Acta Neuropathol 113, 277-293.

Popa-Wagner, A., Buga, A.M., Kokaia, Z., 2011. Perturbed cellular response to brain injury during aging. Ageing Res Rev 10, 71-79.

Sato, K., Hayashi, T., Sasaki, C., Iwai, M., Li, F., Manabe, Y., Seki, T., Abe, K., 2001. Temporal and spatial differences of PSA-NCAM expression between young-adult and aged rats in normal and ischemic brains. Brain Res 922, 135-139.

Shook, B.A., Manz, D.H., Peters, J.J., Kang, S., Conover, J.C., 2012. Spatiotemporal changes to the subventricular zone stem cell pool through aging. J Neurosci 32, 6947-6956.

Sun, F., Wang, X., Mao, X., Xie, L., Jin, K., 2012. Ablation of neurogenesis attenuates recovery of motor function after focal cerebral ischemia in middle-aged mice. PLoS One 7, e46326.

Takasawa, K., Kitagawa, K., Yagita, Y., Sasaki, T., Tanaka, S., Matsushita, K., Ohstuki, T., Miyata, T., Okano, H., Hori, M., Matsumoto, M., 2002. Increased proliferation of neural progenitor cells but reduced survival of newborn cells in the contralateral hippocampus after focal cerebral ischemia in rats. Journal of Cerebral Blood Flow and Metabolism 22, 299-307.

Tang, Y., Wang, J., Lin, X., Wang, L., Shao, B., Jin, K., Wang, Y., Yang, G.-Y., 2014. Neural stem cell protects aged rat brain from ischemia-reperfusion injury through neurogenesis and angiogenesis. Journal of Cerebral Blood Flow and Metabolism 34, 1138-1147.

Tokutomi, T., Miyagi, T., Ogawa, T., Ono, J., Kawamata, T., Sakamoto, T., Shigemori, M., Nakamura, N., 2008. Age-associated increases in poor outcomes after traumatic brain injury: a report from the Japan Neurotrauma Data Bank. J Neurotrauma 25, 1407-1414.

Tropepe, V., Craig, C.G., Morshead, C.M., van der Kooy, D., 1997. Transforming growth factor-alpha null and senescent mice show decreased neural progenitor cell proliferation in the forebrain subependyma. J Neurosci 17, 7850-7859.

Vandeputte, C., Reumers, V., Aelvoet, S.-A., Thiry, I., De Swaef, S., Van den Haute, C., Pascual-Brazo, J., Farr, T.D., Vande Velde, G., Hoehn, M., Himmelreich, U., Van Laere, K., Debyser, Z., Gijsbers, R., Baekelandt, V., 2014. Bioluminescence imaging of stroke-induced endogenous neural stem cell response. Neurobiology of Disease 69, 144-155.

Villeda, S.A., Wyss-Coray, T., 2013. The circulatory systemic environment as a modulator of neurogenesis and brain aging. Autoimmunity Reviews 12, 674-677.

Wang, X., Mao, X., Xie, L., Sun, F., Greenberg, D.A., Jin, K., 2012. Conditional depletion of neurogenesis inhibits long-term recovery after experimental stroke in mice. PLoS One 7, e38932.

Yager, J.Y., Wright, S., Armstrong, E.A., Jahraus, C.M., Saucier, D.M., 2006. The influence of aging on recovery following ischemic brain damage. Behav Brain Res 173, 171-180.

Figure 1

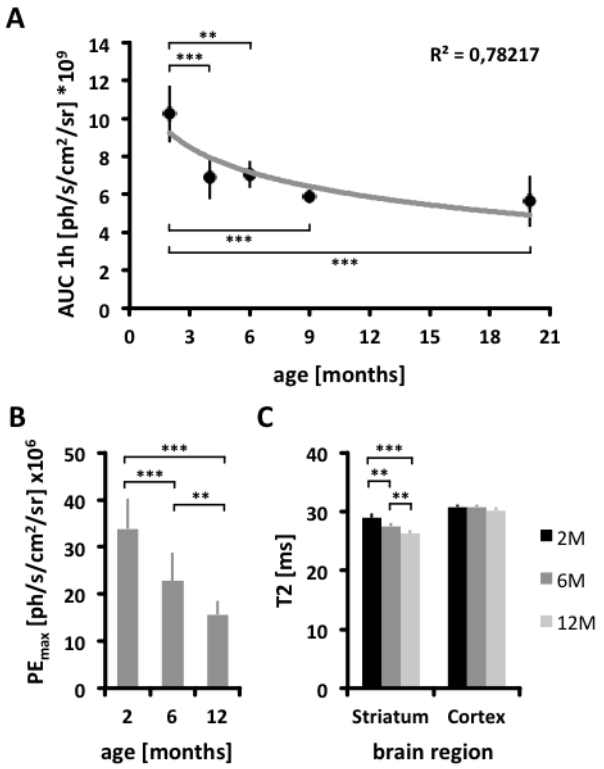

Figure 2

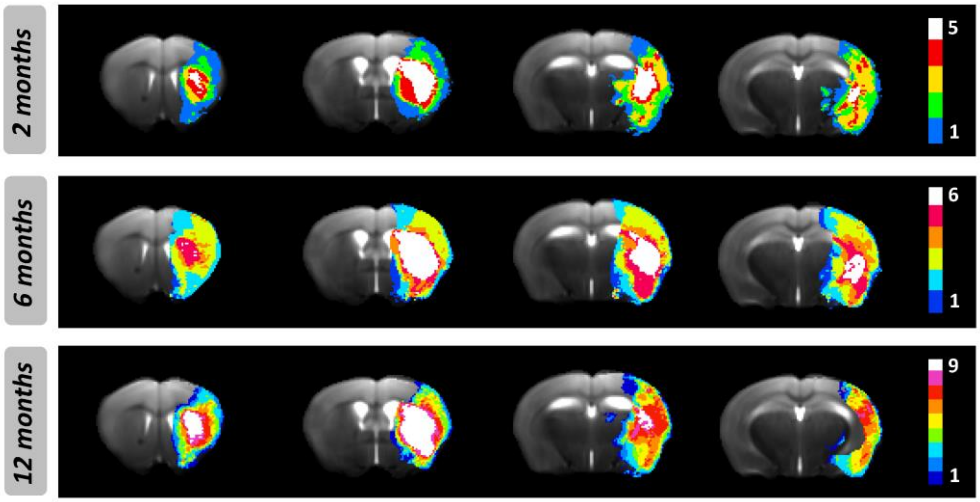

Figure 3

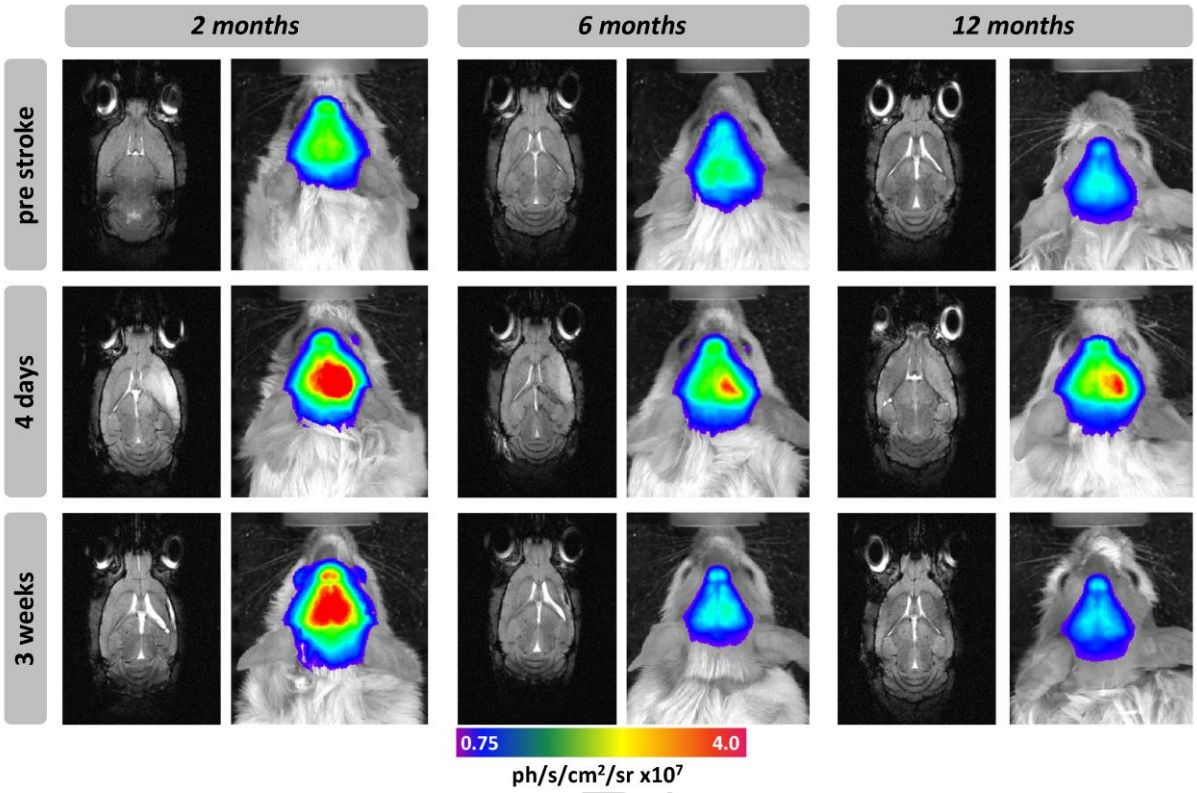

Figure 4

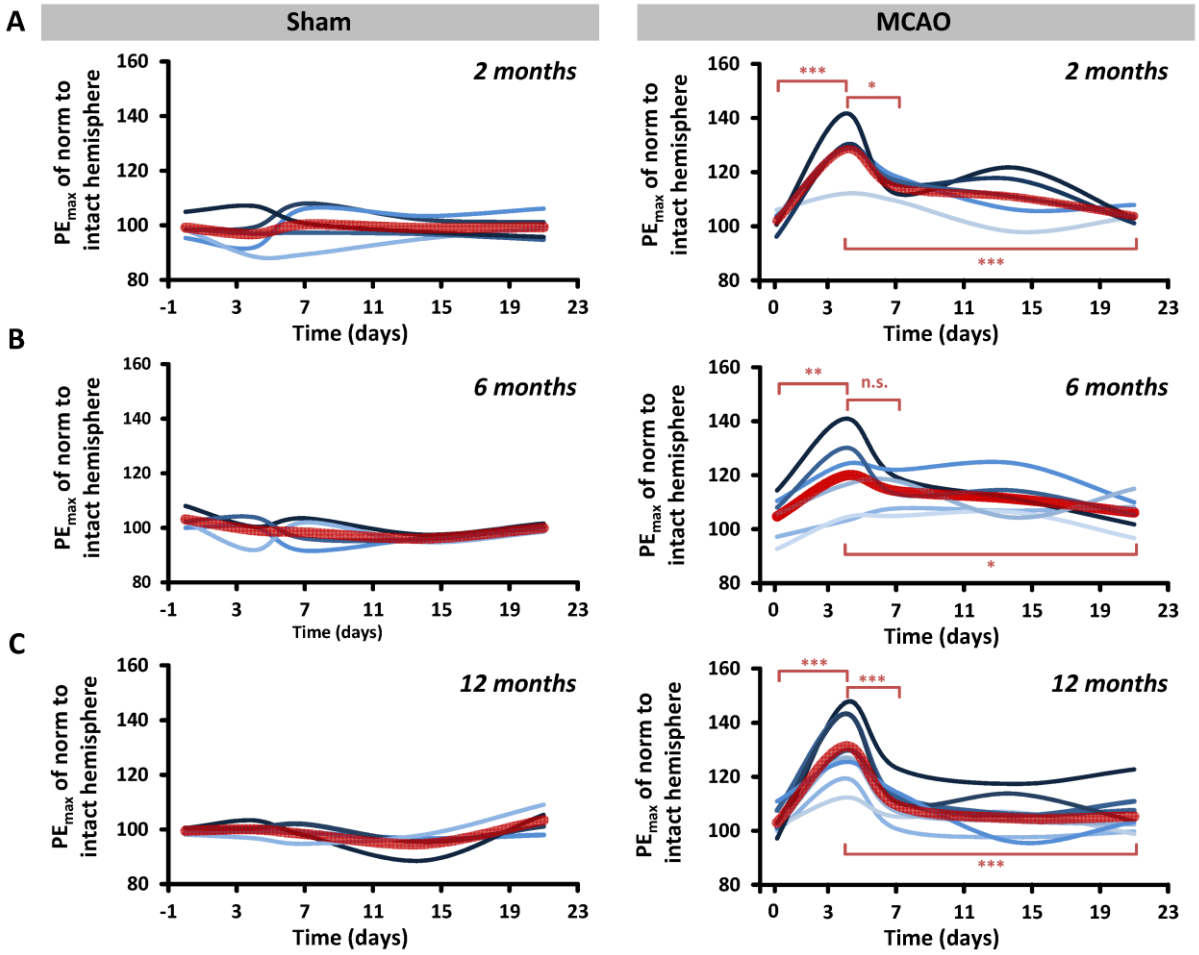

Figure 5

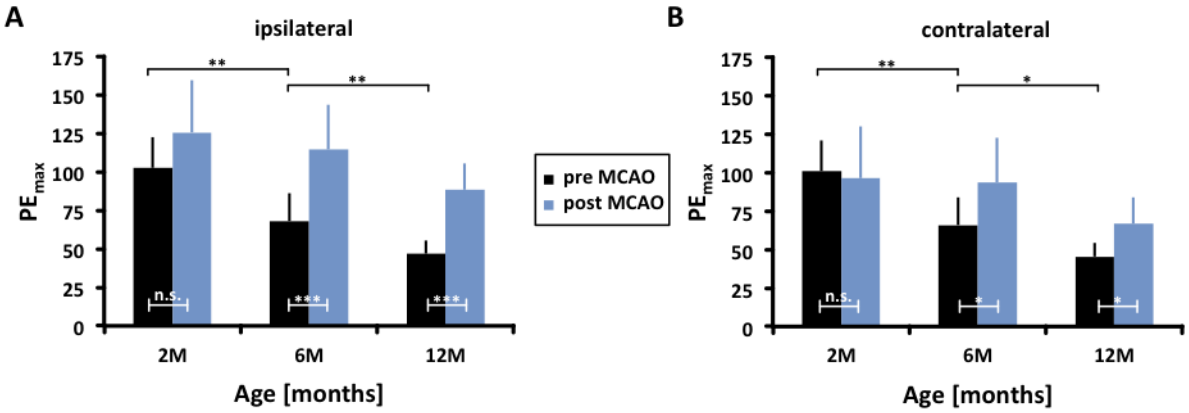

Figure 6

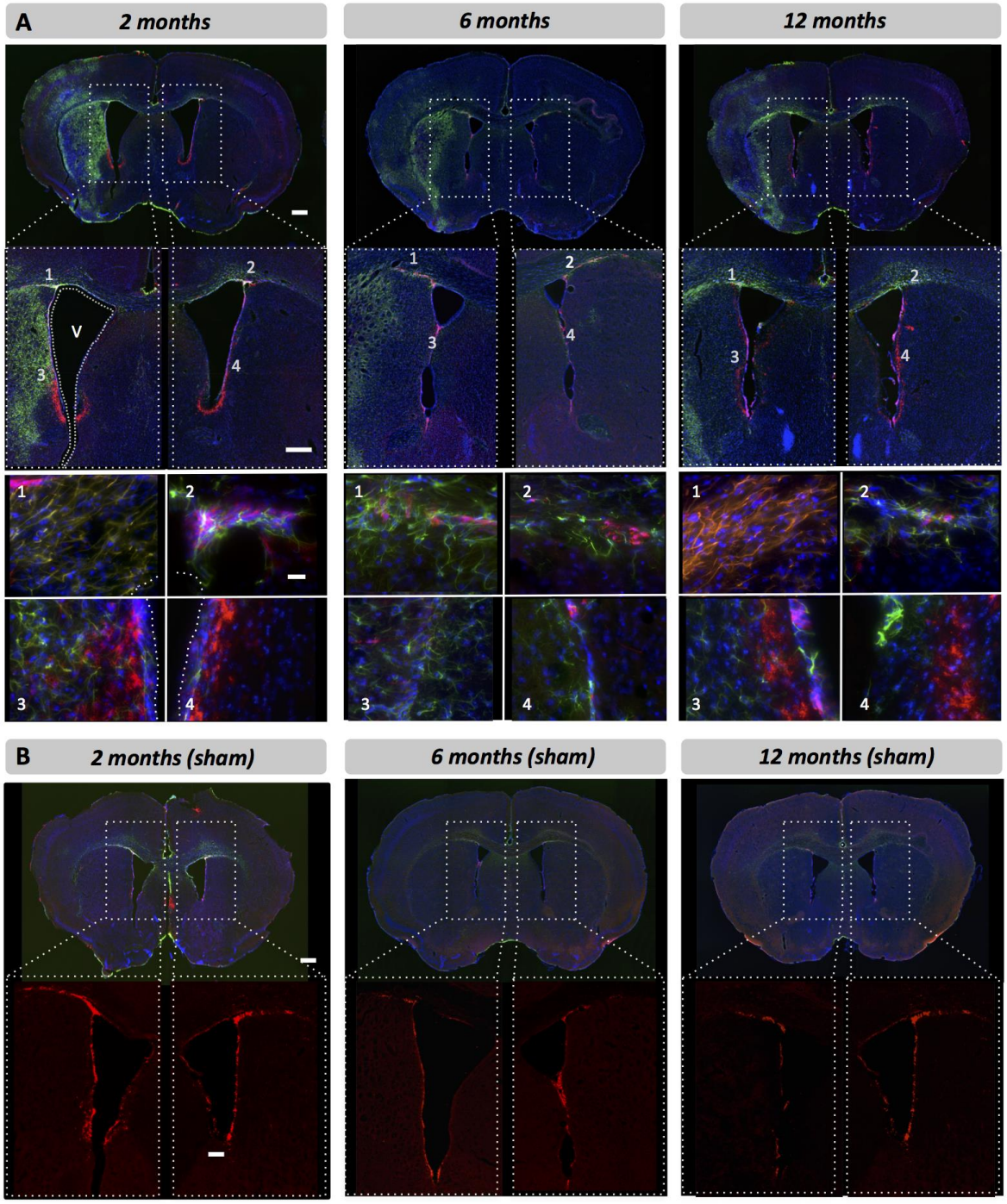

Figure 7

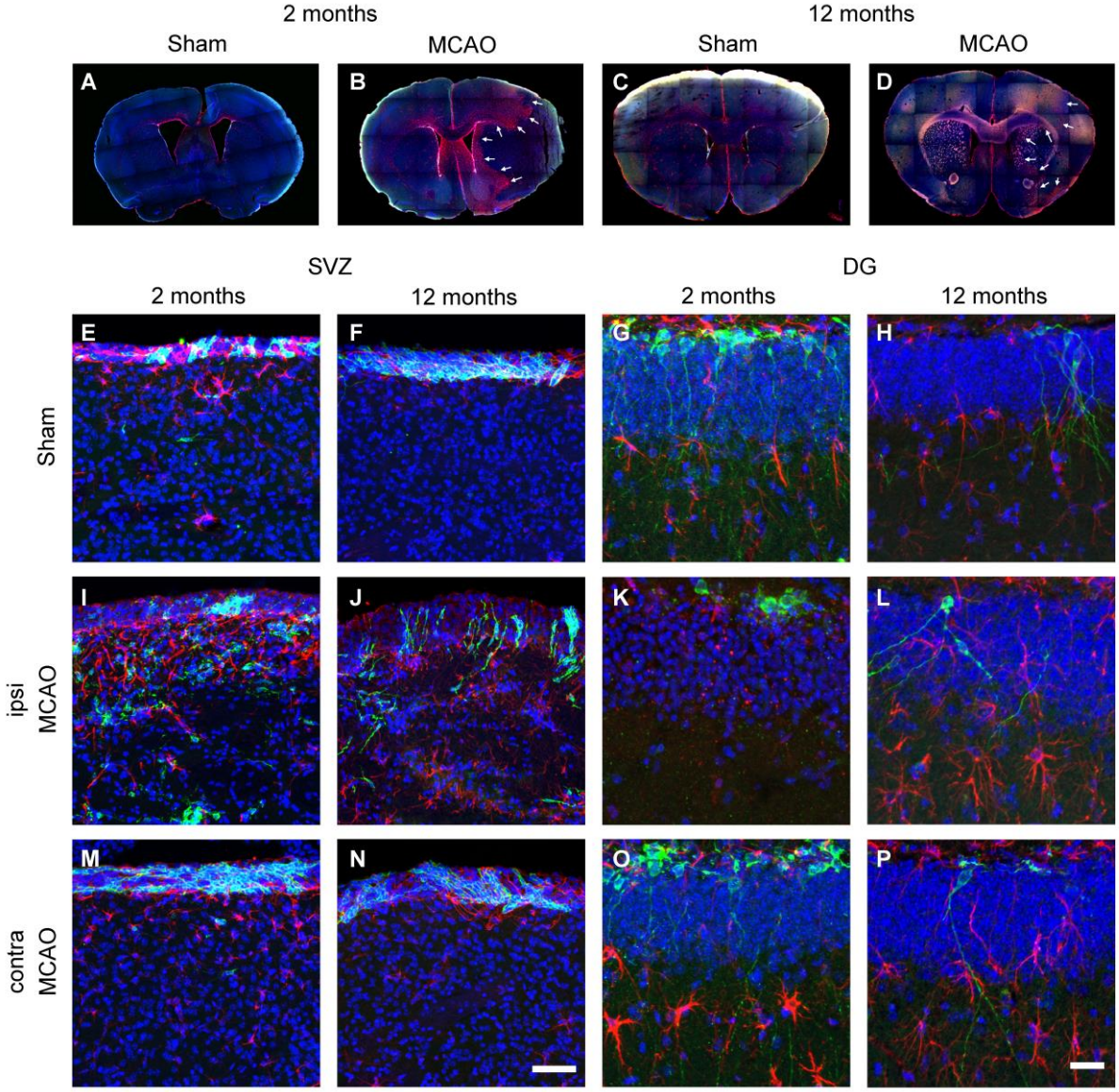

Highlights:

- Optical imaging of the transgenic mouse DCX-Luc monitors spontaneous upregulation of neurogenesis after stroke efficiently
- Neurogenesis, hence the number of DCX+ cells, is upregulated upon stroke independent of age with a peak at day 4 and return to baseline levels 21 days post stroke
- Older animals effectively compensate for reduced basal neurogenesis by an enhanced sensitivity to the cerebral lesion